Supporting Information

$IrO_2/LiLa_2IrO_6$ as a Robust Electrocatalyst for Oxygen Evolution Reaction in Acidic Media

HuiHui Liu[‡a], Haeseong Jang[‡b], Yu Wang[a], Min Gyu Kim[c], Haisen Li[a], Qing Qin*[a], Xien Liu*[a], Jaephil Cho*[b]

[a]College of Chemical Engineering, Qingdao University of Science and Technology, Qingdao 266042, P. R. China

[b]Department of Energy Engineering, Department of Energy and Chemical Engineering, Ulsan National Institute of Science and Technology (UNIST), Ulsan 44919, South Korea

[c]Beamline Research Division, Pohang Accelerator Laboratory (PAL), Pohang 37673, South Korea

[‡]These authors contributed equally to this work

*E-mail addresses: qinqing@qust.edu.cn (Q. Qin); liuxien@qust.edu.cn (X. Liu); jpcho@unist.ac.kr (J. Cho)

List of Contents

Fig. S9. The XRD pattern of catalyst prepared with an annealing temperature of 1000 ^{o}C.

Fig. S10. The Nyquist plots for catalysts prepared with different annealing temperature (from 1000 ^{o}C to 1200 ^{o}C).

Fig. S11. The CV curves recorded at different scan rates for the catalysts prepared with different molar ratio of Li to La to determine the double layer capacitance: a) Li: La=1:1, b) Li: La=1:2, c) Li: La=1:4, d) Li: La=2:1.

Supplementary Table S1. Comparison of the overpotentials at 10 mA cm^{-2} with recently reported OER catalysts in acidic electrolytes.

Experimental sections

1. Reagents

A solid phase synthesis method was adopted that used following reagents: $C_6H_9O_6La \cdot xH_2O$ (M: 245.09, 99.9 %), and $IrCl_4 \cdot xH_2O$ (M: 334.03, Ir 48.0 - 55.0 %) were purchased from Aladdin, and LiCl (M: 42.39, 99.0 %), and commercial IrO_2 (99.9 %) were purchased from Macklin

2. Synthesis of materials

In a simple procedure, 1.7 mg of the LiCl, 50.7 mg of the $C_6H_9O_6La \cdot xH_2O$ and 33.4 mg of the $IrCl_4 \cdot xH_2O$ were fully ground in an agate mortar to obtain a uniform solid powder. Then, the solid powder was put into a corundum crucible and moved into a muffle furnace, and heated to 1200 °C with a heating rate of 2 °C min^{-1} under the ambient air. After annealed for 4 hours, the target products were collected for electrochemical testing. In order to investigate the effects of reaction temperature and different ratios of lithium to lanthanum on the catalytic performance of the catalyst, a series of experiments related to temperature and the ratio of lithium to lanthanum were carried out.

3. Materials characterization

The powder X-ray diffraction of the prepared catalysts were analyzed with D/Max200, Rigaku diffraction system using Cu-Kα radiation with 2θ range of 10 – 80^o. The morphology and size of catalysts were characterized by the scanning electron microscope (Hitachi S-4800). TEM and HRTEM measurements were performed on the JEOL JEM-2100F transmission electron microscope. Thermo Scientific ESCALAB

250Xi X-ray photoelectron spectrometer was used to measure the XPS spectra. The XANES and EXAFS were recorded at room temperature by the BL10c beam line at the Pohang Light Source (PLS-II), Korea.

4. Electrocatalytic measurements

The catalytic oxygen evolution reaction performance of the prepared catalysts were investigated in a standard three-electrode cell in 0.1 M $HClO_4$ solution. The cell consists of a glassy carbon working electrode (GC electrode, 3 mm in diameter), a reversible hydrogen reference electrode, and a carbon rod counter electrode. The working electrodes were prepared by loading 5 μL of catalyst ink onto glassy carbon (GC) electrode. The catalyst ink was prepared by uniformly dispersing 2 mg of catalyst $IrO_2/LiLa_2IrO_6$, 40 μL of 5 wt % Nafion solution (Sigma-Aldrich, 5 wt%) and 0.4 mg of XC-72 conductive carbon into a mixture of 100 μL of deionized water and 200 μL of anhydrous ethanol by ultrasounding for 30 minutes. The polarization curves were measured with a scan rate of 5 mV s^{-1}, and the potential range was 1.0 - 1.65 (V vs RHE). All data were obtained with IR (95 %) compensation. The ESI measurements were carried out at the open circuit potential in the frequency range of 100 kHz - 0.01 Hz. The durability tests were conducted by a chronopotentiometry method at a constant current density of 10 mA cm^{-2}. In order to improve the electrochemical stability, a Titanium mesh (1*1 cm^2) with loading of 150 μL catalyst ink was used as the working electrode during the durability testing.

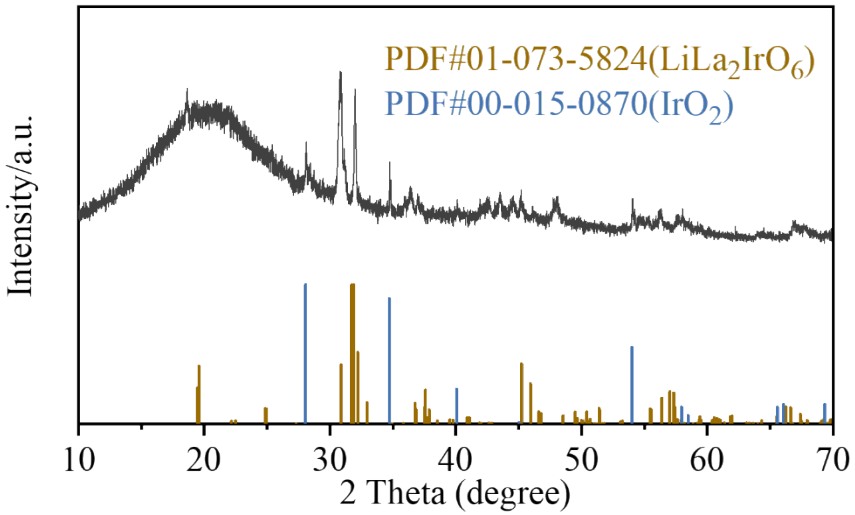

Fig. S1. The XRD pattern of the $IrO_2/LiLa_2IrO_6$.

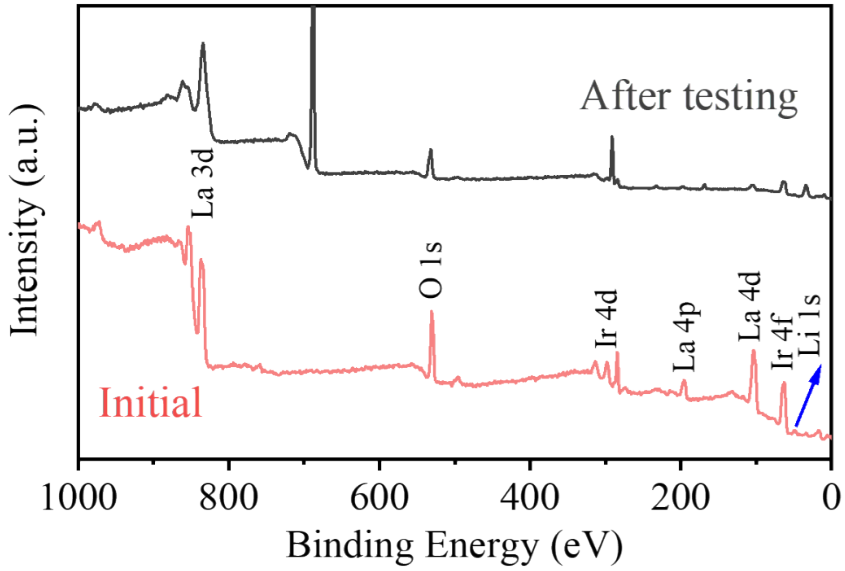

Fig. S2. The XPS survey spectra of the $IrO_2/LiLa_2IrO_6$ before and after OER testing.

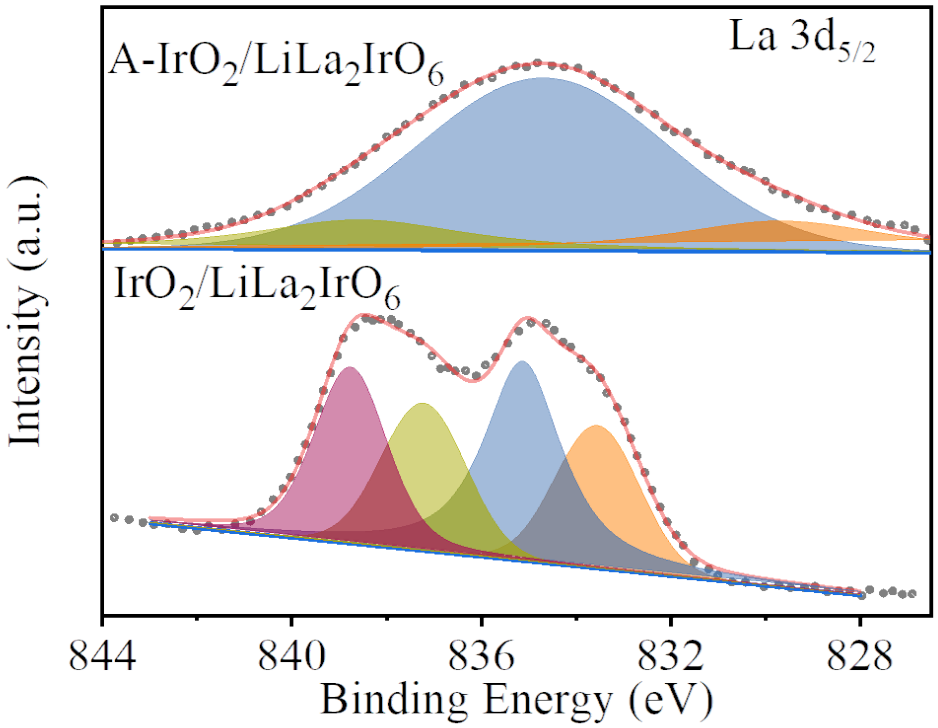

Fig. S3. The high-resolution XPS spectra of the La 3d for the $IrO_2/LiLa_2IrO_6$ and A-$IrO_2/LiLa_2IrO_6$ (A refers to the samples collected after OER testing).

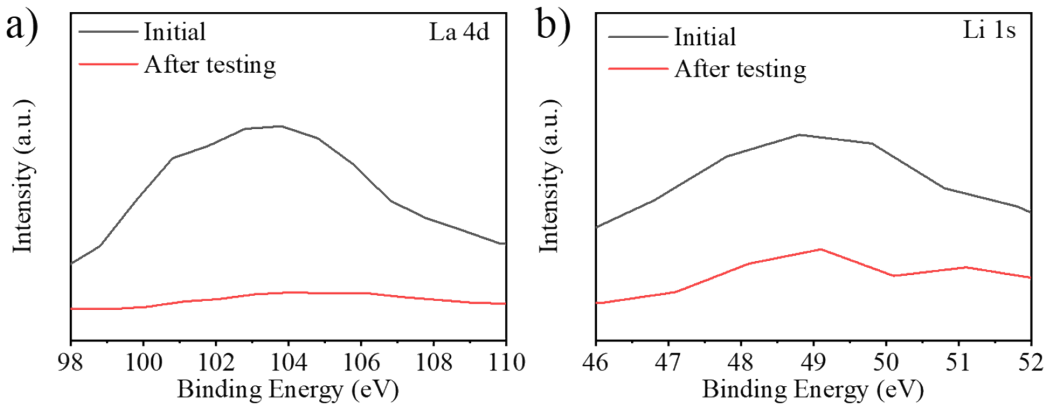

Fig. S4. The high-resolution XPS spectra of the $IrO_2/LiLa_2IrO_6$ before and after testing: a) La 4d, b) Li 1s.

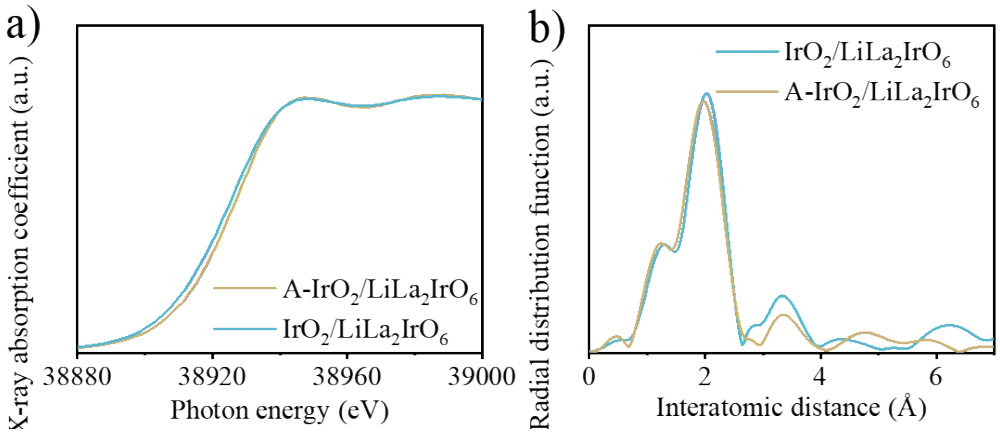

Fig. S5. a) K-edge XANES spectra of La for $IrO_2/LiLa_2IrO_6$ and A-$IrO_2/LiLa_2IrO_6$, b) The corresponding k^3-weighted Fourier transforms of La K-edge EXAFS spectra for $IrO_2/LiLa_2IrO_6$ and A-$IrO_2/LiLa_2IrO_6$.

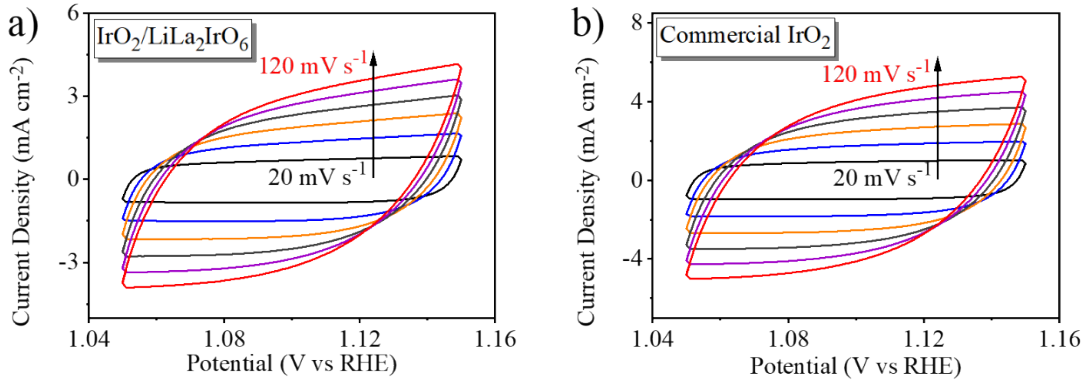

Fig. S6. The CV curves recorded at different scan rates for a) $IrO_2/LiLa_2IrO_6$, b) Commercial IrO_2 in a non-Faradaic potential window from 1.05 - 1.15 V (vs RHE).

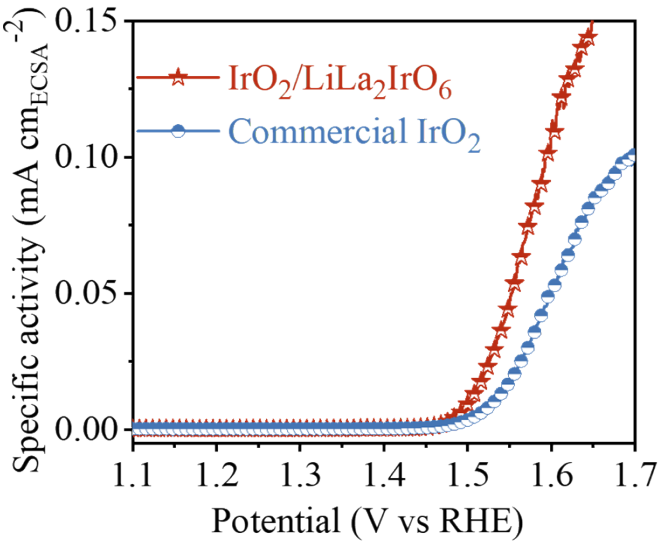

Fig. S7. The specific activity (normalized to the ECSA) of $IrO_2/LiLa_2IrO_6$ and IrO_2.

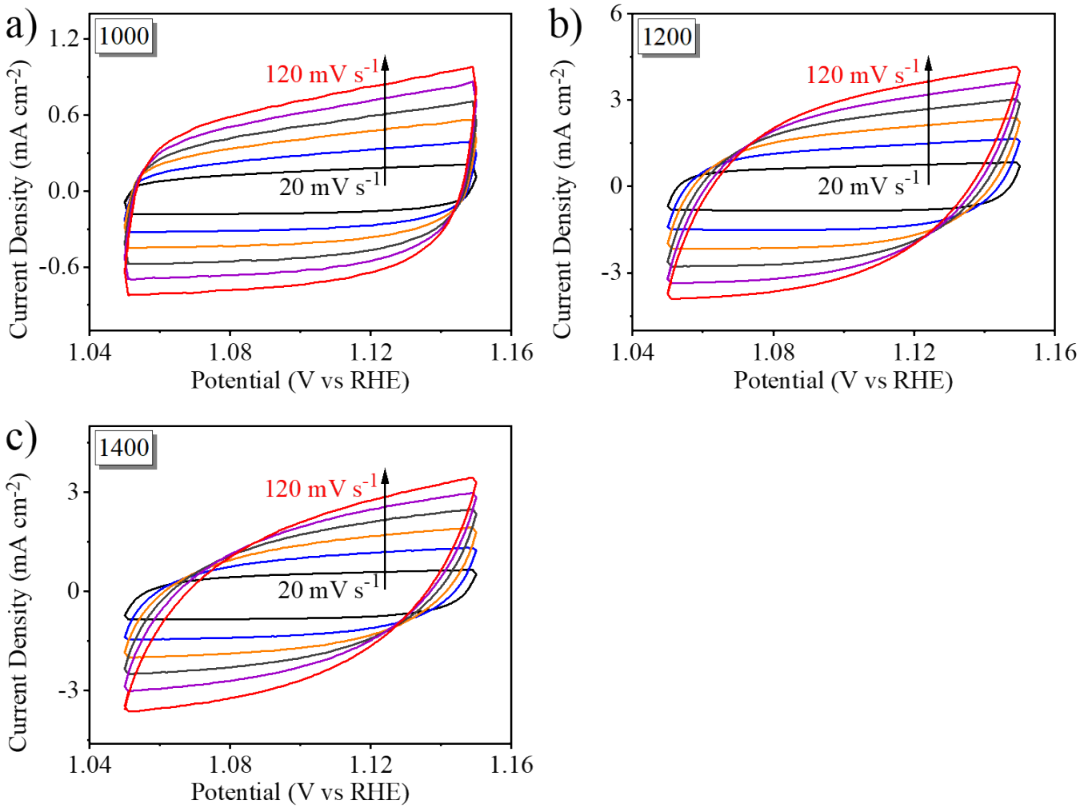

Fig. S8. The CV curves recorded at different scan rates for catalysts prepared with different annealing temperature: a) 1000 °C, b) 1200 °C, c) 1400 °C in a non-Faradaic potential window from 1.05 - 1.15 V (vs RHE).

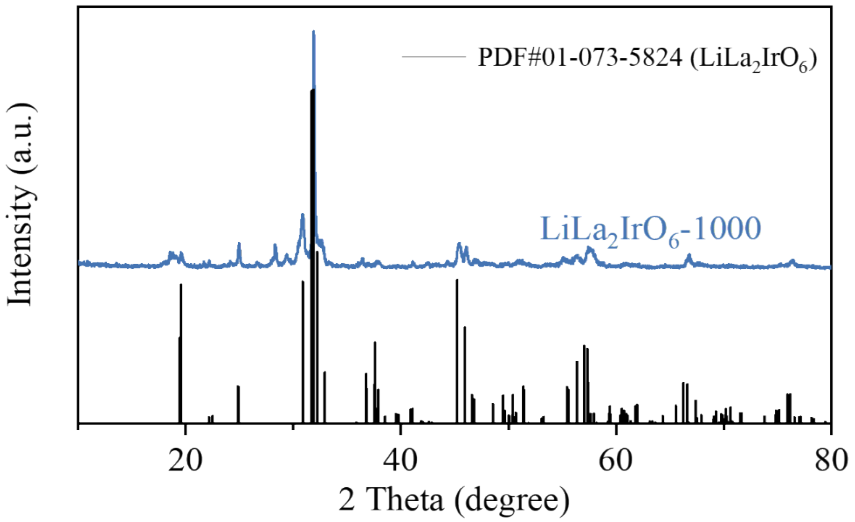

Fig. S9. The XRD pattern of catalyst prepared with an annealing temperature of 1000 ^{o}C.

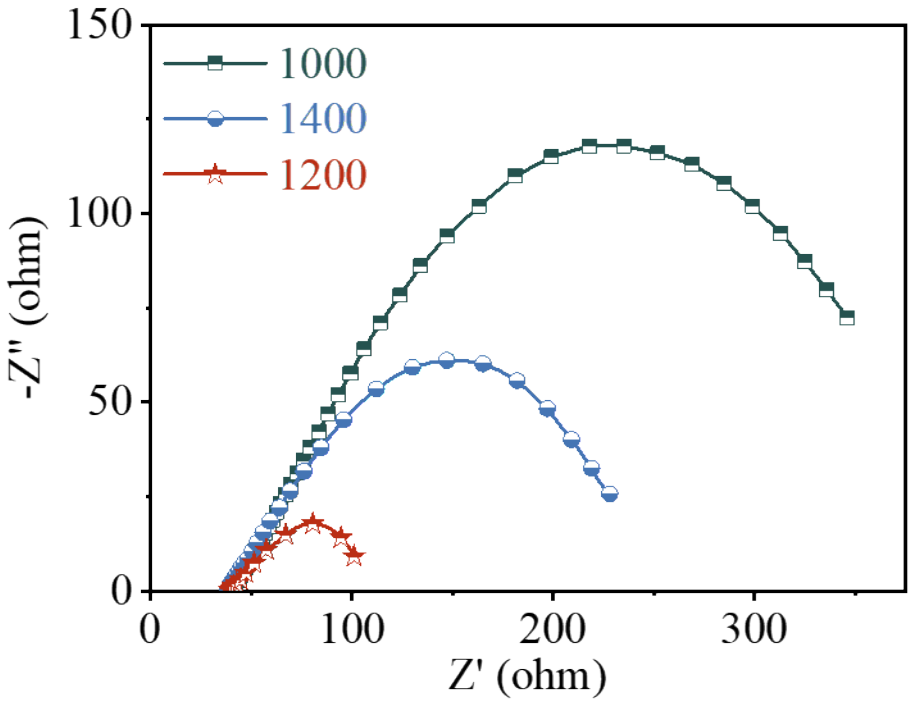

Fig. S10. The Nyquist plots for catalysts prepared with different annealing temperature (from 1000 ºC to 1200 ºC).

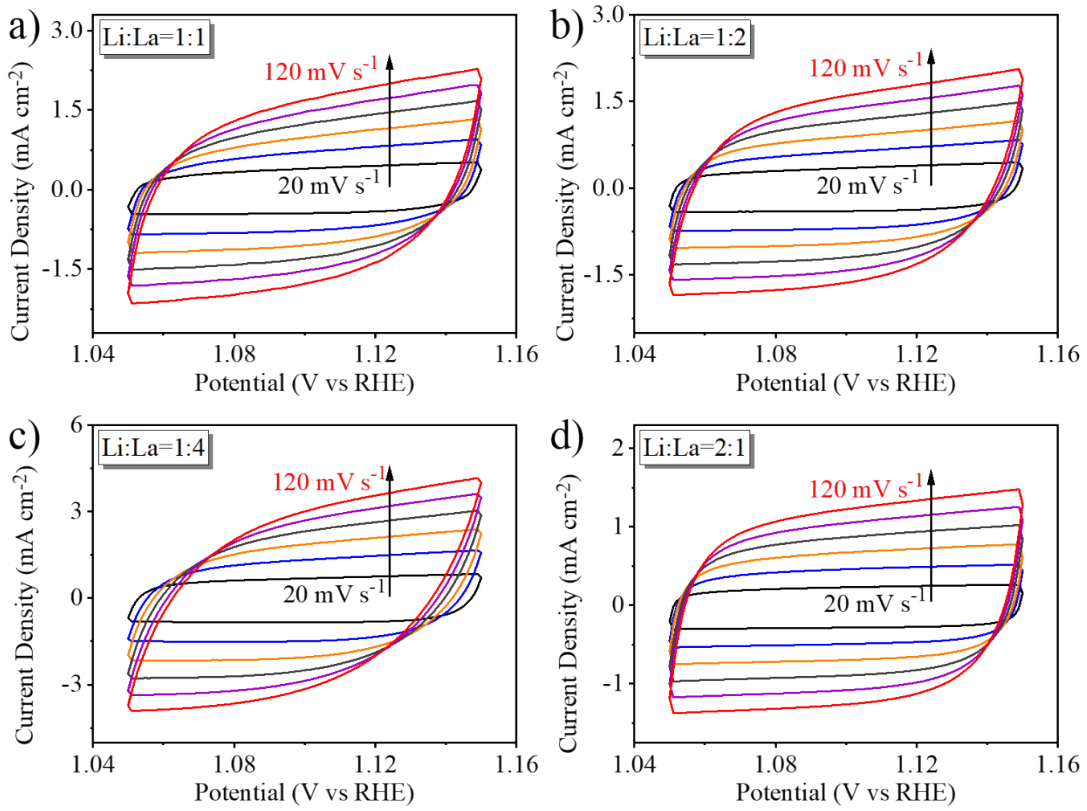

Fig. S11. The CV curves recorded at different scan rates for the catalysts prepared with different molar ratio of Li to La to determine the double layer capacitance: a) Li: La = 1 : 1, b) Li: La = 1 : 2, c) Li: La = 1 : 4, d) Li: La = 2 : 1.

Supplementary Table S1. Comparison of the overpotentials at 10 mA cm^{-2} with recently reported OER catalysts in acidic electrolytes.

Catalysts	Electrolyte	Overpotential (mV) at 10 mA cm^{-2}	References
3D Ir superstructures	0.1 M $HClO_4$	270	[1]
$Y_{2-x}Ca_xRu_2O_{7-\delta}$	0.5 M H_2SO_4	275	[2]
$IrO_2/LiLa_2IrO_6$	0.1 M $HClO_4$	278	This work
Ru @IrO_x	0.05 M H_2SO_4	282	[3]
$Y_{2-x}Zn_xRu_2O_7$	0.5 M H_2SO_4	291	[4]
La_3IrO_7-SLD	0.1 M $HClO_4$	296	[5]
Ir-Ni	0.1 M $HClO_4$	300	[6]
$BaIrO_3$	0.5 M H_2SO_4	300	[7]
IrCoNi/C	0.1 M $HClO_4$	303	[8]
Pr_3IrO_7	0.1 M $HClO_4$	305	[9]
$IrCu_{2.3}$ nanocrystal	0.05 M H_2SO_4	310	[10]
IrNi-RFs	0.1 M $HClO_4$	314	[11]
Ir/Fe_4N	0.5 M H_2SO_4	316	[12]
SnO_2-Sb-IrO_2	0.5 M H_2SO_4	318	[13]
FeNC	0.5 M H_2SO_4	320	[14]
0.5IrO_2-0.5SiO_2	0.5 M H_2SO_4	322	[15]
Ba_2YIrO_6	0.1 M $HClO_4$	330	[16]
$IrNiO_x$/ATO	0.05 M H_2SO_4	330	[17]
$Ir_{0.7}Co_{0.3}O_x$	0.5 M H_2SO_4	330	[18]
OEEG	0.5 M H_2SO_4	334	[19]

$SrCo_{0.9}Ir_{0.1}O_{3-\delta}$	0.1 M $HClO_4$	340	[20]
IrOOH	0.1 M $HClO_4$	344	[21]
$Cu_{0.3}Ir_{0.7}O_{\delta}$	0.1 M $HClO_4$	350	[22]
Ir_2SnO_x	0.5 M H_2SO_4	355	[23]
Ti/IrO_2	0.5 M H_2SO_4	361	[24]
$W_{0.57}Ir_{0.43}O_{3-\delta}$	1 M H_2SO_4	370	[25]
Ba[3]/CPO	0.5 M H_2SO_4	385	[26]
CN_x	0.1 M $HClO_4$	390	[27]
Sr_2FeIrO_6	0.1 M $HClO_4$	400	[28]
$Sr_2Fe_{0.5}Ir_{0.5}O_4$	0.1 M $HClO_4$	400	[28]
Ir_7Au	0.1 M $HClO_4$	410	[29]

References:

[1] Y. Pi, N. Zhang, S. Guo, J. Guo, X. Huang, Ultrathin Laminar Ir Superstructure as Highly Efficient Oxygen Evolution Electrocatalyst in Broad pH Range, Nano Letters, 16 (2016) 4424-4430.

[2] Q. Feng, Z. Zhao, X. Z. Yuan, H. Li, H. Wang, Oxygen Vacancy Engineering of Yttrium Ruthenate Pyrochlores as an Efficient Oxygen Catalyst for Both Proton Exchange Membrane Water Electrolyzers and Rechargeable Zinc-air Batteries, Applied Catalysis B: Environmental, 260 (2020) 118176.

[3] J. Shan, C. Guo, Y. Zhu, S. Chen, L. Song, M. Jaroniec, Y. Zheng, S. Z. Qiao, Charge-Redistribution-Enhanced Nanocrystalline Ru@IrO_x Electrocatalysts for Oxygen Evolution in Acidic Media, Chem, 5 (2019) 445-459.

[4] Q. Feng, Q. Wang, Z. Zhang, Y. Xiong, H. Li, Y. Yao, X.-Z. Yuan, M.C. Williams, M. Gu, H. Chen, H. Li, H. Wang, Highly Active and Stable Ruthenate Pyrochlore for Enhanced Oxygen Evolution Reaction in Acidic Medium Electrolysis, Applied Catalysis B: Environmental, 244 (2019) 494-501.

[5] Q. Qin, H. Jang, Y. Wang, L. Zhang, Z. Li, M.G. Kim, S. Liu, X. Liu, J. Cho, Gettering La Effect from La_3IrO_7 as a Highly Efficient Electrocatalyst for Oxygen Evolution Reaction in Acid Media, Advanced Energy Materials, 11 (2021) 2003561.

[6] T. Reier, Z. Pawolek, S. Cherevko, M. Bruns, T. Jones, D. Teschner, S. Selve, A. Bergmann, H.N. Nong, R. Schlögl, K.J.J. Mayrhofer, P. Strasser, Molecular Insight in Structure and Activity of Highly Efficient, Low-Ir Ir-Ni Oxide Catalysts for Electrochemical Water Splitting (OER), Journal of the American Chemical Society,

137 (2015) 13031-13040.

[7] C.W. Song, H. Suh, J. Bak, H.B. Bae, S.-Y. Chung, Dissolution-Induced Surface Roughening and Oxygen Evolution Electrocatalysis of Alkaline-Earth Iridates in Acid, Chem, 5 (2019) 3243-3259.

[8] J. Feng, F. Lv, W. Zhang, P. Li, K. Wang, C. Yang, B. Wang, Y. Yang, J. Zhou, F. Lin, G.-C. Wang, S. Guo, Iridium-Based Multimetallic Porous Hollow Nanocrystals for Efficient Overall-Water-Splitting Catalysis, Advanced Materials, 29 (2017) 1703798.

[9] Y. Wang, S. Liu, Q. Qin, H. Liu, L. Zhang, T. Wei, H. Li, X. Liu, Praseodymium Iridium Oxide as a Competitive Electrocatalyst for Oxygen Evolution Reaction in Acid Media, Science China Materials, (2021).

[10] Y. Pi, J. Guo, Q. Shao, X. Huang, Highly Efficient Acidic Oxygen Evolution Electrocatalysis Enabled by Porous Ir-Cu Nanocrystals with Three-Dimensional Electrocatalytic Surfaces, Chemistry of Materials, 30 (2018) 8571-8578.

[11] H. Jin, Y. Hong, J. Yoon, A. Oh, N.K. Chaudhari, H. Baik, S.H. Joo, K. Lee, Lanthanide Metal-Assisted Synthesis of Rhombic Dodecahedral MNi (M = Ir and Pt) Nanoframes toward Efficient Oxygen Evolution Catalysis, Nano Energy, 42 (2017) 17-25.

[12] B.M. Tackett, W. Sheng, S. Kattel, S. Yao, B. Yan, K.A. Kuttiyiel, Q. Wu, J.G. Chen, Reducing Iridium Loading in Oxygen Evolution Reaction Electrocatalysts Using Core-Shell Particles with Nitride Cores, ACS Catalysis, 8 (2018) 2615-2621.

[13] J. Tong, Y. Liu, Q. Peng, W. Hu, Q. Wu, An Efficient Sb-SnO_2-Supported IrO_2

Electrocatalyst for the Oxygen Evolution Reaction in Acidic Medium, Journal of Materials Science, 52 (2017) 13427-13443.

[14] K. Mamtani, D. Jain, A.C. Co, U.S. Ozkan, Nitrogen-Coordinated Iron−Carbon as Efficient Bifunctional Electrocatalysts for the Oxygen Reduction and Oxygen Evolution Reactions in Acidic Media, Energy & Fuels, 31 (2017) 6541-6547.

[15] J.-J. Zhang, J.-M. Hu, J.-Q. Zhang, C.-N. Cao, IrO_2–SiO_2 Binary Oxide Films: Geometric or Kinetic Interpretation of the Improved Electrocatalytic Activity for the Oxygen Evolution Reaction, International Journal of Hydrogen Energy, 36 (2011) 5218-5226.

[16] O. Diaz-Morales, S. Raaijman, R. Kortlever, P.J. Kooyman, T. Wezendonk, J. Gascon, W.T. Fu, M.T.M. Koper, Iridium-Based Double Perovskites for Efficient Water Oxidation in Acid Media, Nature Communications, 7 (2016) 12363.

[17] H.N. Nong, H.-S. Oh, T. Reier, E. Willinger, M.-G. Willinger, V. Petkov, D. Teschner, P. Strasser, Oxide-Supported $IrNiO_x$ Core-Shell Particles as Efficient, Cost-Effective, and Stable Catalysts for Electrochemical Water Splitting, Angewandte Chemie International Edition, 54 (2015) 2975-2979.

[18] W. Hu, H. Zhong, W. Liang, S. Chen, Ir-Surface Enriched Porous Ir-Co Oxide Hierarchical Architecture for High Performance Water Oxidation in Acidic Media, ACS Applied Materials & Interfaces, 6 (2014) 12729-12736.

[19] C. Lei, Q. Zheng, F. Cheng, Y. Hou, B. Yang, Z. Li, Z. Wen, L. Lei, G. Chai, X. Feng, High-Performance Metal-Free Nanosheets Array Electrocatalyst for Oxygen Evolution Reaction in Acid, Advanced Functional Materials, 30 (2020) 2003000.

[20] Y. Chen, H. Li, J. Wang, Y. Du, S. Xi, Y. Sun, M. Sherburne, J.W. Ager, A.C. Fisher, Z.J. Xu, Exceptionally Active Iridium Evolved from a Pseudo-Cubic Perovskite for Oxygen Evolution in Acid, Nature Communications, 10 (2019) 572.

[21] D. Weber, L.M. Schoop, D. Wurmbrand, S. Laha, F. Podjaski, V. Duppel, K. Müller, U. Starke, B.V. Lotsch, IrOOH Nanosheets as Acid Stable Electrocatalysts for the Oxygen Evolution Reaction, Journal of Materials Chemistry A, 6 (2018) 21558-21566.

[22] W. Sun, Y. Song, X.-Q. Gong, L.-m. Cao, J. Yang, An Efficiently Tuned D-orbital Occupation of IrO_2 by Doping with Cu for Enhancing the Oxygen Evolution Reaction Activity, Chemical Science, 6 (2015) 4993-4999.

[23] W.T. Lu, P. Yuan, F. Wei, K. Cheng, W.H. Li, Y.H. Zhou, W.Q. Zheng, G. Zhang, Porous Ir-Sn Binary Oxide Nanorod Assembly as an Efficient Electrocatalyst for Water Oxidation, International Journal of Electrochemical Science, 13 (2018) 3235-3245.

[24] Y. Xie, Y. Deng, C. Yang, Z. Zeng, Y. Li, G. Chen, CoO_x Functionalized IrO_2-Sb_2O_5-SnO_2 Anode with an Enhanced Activity and Stability for Electrocatalytic Oxygen Evolution, Journal of Alloys and Compounds, 696 (2017) 257-265.

[25] S. Kumari, B.P. Ajayi, B. Kumar, J.B. Jasinski, M.K. Sunkara, J.M. Spurgeon, A Low-Noble-Metal $W_{1-x}Ir_xO_{3-\delta}$ Water Oxidation Electrocatalyst for Acidic Media Via Rapid Plasma Synthesis, Energy & Environmental Science, 10 (2017) 2432-2440.

[26] X.-B. Han, D.-X. Wang, E. Gracia-Espino, Y.-H. Luo, Y.-Z. Tan, D.-F. Lu, Y.-G. Li, T. Wagberg, E.-B. Wang, L.-S. Zheng, Fe-Substituted Cobalt-Phosphate Polyoxometalates as Enhanced Oxygen Evolution Catalysts in Acidic Media, Chinese

Journal of Catalysis, 41 (2020) 853-857.

[27] K. Mamtani, D. Jain, D. Dogu, V. Gustin, S. Gunduz, A.C. Co, U.S. Ozkan, Insights into Oxygen Reduction Reaction (ORR) and Oxygen Evolution Reaction (OER) Active Sites for Nitrogen-Doped Carbon Nanostructures (CN_x) in Acidic Media, Applied Catalysis B: Environmental, 220 (2018) 88-97.

[28] R. Zhang, N. Dubouis, M. Ben Osman, W. Yin, M.T. Sougrati, D.A.D. Corte, D. Giaume, A. Grimaud, A Dissolution/Precipitation Equilibrium on the Surface of Iridium-Based Perovskites Controls Their Activity as Oxygen Evolution Reaction Catalysts in Acidic Media, Angewandte Chemie International Edition, 58 (2019) 4571-4575.

[29] S.H. Ahn, H. Tan, M. Haensch, Y. Liu, L.A. Bendersky, T.P. Moffat, Self-Terminated Electrodeposition of Iridium Electrocatalysts, Energy & Environmental Science, 8 (2015) 3557-3562.